

## Dynamic Response Analysis of Middle Pillar for Ultra-small Spacing Tunnels under Train Vibration Loads

Shuren Wang<sup>1, 2,\*</sup>, Kunpeng Shi<sup>1</sup>, Yongsheng He<sup>3</sup> and Xinquan Wang<sup>4</sup>

<sup>1</sup>International Joint Research Laboratory of Henan Province for Underground Space Development and Disaster Prevention, Henan Polytechnic University, Jiaozuo 454003, China

<sup>2</sup>School of Minerals and Energy Resources Engineering, University of New South Wales, Sydney, NSW 2052, Australia

<sup>3</sup>Institute of National Defense Engineering, Academy of Military Sciences, Luoyang 471023, China

<sup>4</sup>School of Engineering, Zhejiang University City College, Hangzhou 310015, China

Received 7 March 2019; Accepted 15 July 2019

### Abstract

The ultra-small spacing tunnels are widely used in the urban subway. However, due to the narrow and unstable of the middle pillar of the ultra-small spacing tunnels, these tunnels are easy to be damaged under the vibration loads of train. To ensure the middle pillar stability of the ultra-small spacing tunnels, taking Gangding-Shipaiqiao ultra-small spacing tunnels (0-200 mm) on Guangzhou Metro Line 3 in China as engineering background, the dynamic response characteristics of middle pillar under different speeds of single (double) trains in different cross-section types tunnels were analyzed by using ABAQUS. The superposition coefficient of train vibration excitation expression was proposed, and the fitting vibration equations of three different train speeds were obtained, which mainly involved the vertical acceleration, vertical velocity, vertical displacement and horizontal displacement of the middle pillar. Results show that the higher the speed of the train, the greater the influence on the middle pillar. Compared with the asymmetric tunnel section, the symmetrical tunnel section has less influence on the middle pillar, especially on the dynamic response of the horizontal displacement. The conclusions obtained in this work provide reference value for the design and construction of ultra-small spacing tunnels.

*Keywords:* Double-track tunnel, Ultra-small spacing, Dynamic response, Middle pillar

### 1. Introduction

Currently, the traffic vibration has been listed as one of the major environmental hazards in the world [1]. The structural vibration caused by high-speed trains propagates through the surrounding filed or the ground, further induced secondary vibration and noise of nearby underground and adjacent structures. Traffic vibration will have a great impact on the structural safety of the building and the daily life of the residents [2].

Although the vibration amplitude and damage of the surrounding environment caused by the high-speed trains are often small compared with the earthquake, due to the long-term existence of this vibration, this persistent small amplitude vibration will cause the strength and durability of the tunnel structure to decrease. The structure is prone to cracks and even cracking, which will eventually endanger the overall stability and operational safety of the tunnel structure. So, it is an urgent need for setting the potential hazards caused by the middle pillars of ultra-small spacing tunnels under the train vibration loads [3].

Due to urban underground resource shortage and complicated geological conditions, more and more ultra-small spacing tunnels are used in underground engineering. It will be of great significance to study the dynamic response

characteristics of the middle pillar of the ultra-small spacing tunnels under train vibration loads.

### 2. State of the art

Aiming at the dynamic response of the middle pillar for the small spacing tunnels under train vibration loads, many scholars have done lots of researches on the theoretical analysis, simulation calculation and engineering application. It is generally believed that the train speed, track structure, smoothness of train operation, and axle load have a great influence on the stability of the tunnel surrounding rock, supporting structure and middle pillars [4-5].

In case of high-speed rail, according to the numerical modelling and theoretical analysis, the artificial excitation formula to simulate the vertical vibration load was proposed. Considering the mechanism of vibration load generation, the existing formula of train load was rectified and perfected, which laid a foundation for further study of the dynamic response of the surrounding rock and adjacent structures under train vibration loads [6-8]. In addition, the faster the train run, the tunnel structure would produce the greater vibration load and the more obvious acceleration response [9-10]. Yi et al. found that the cumulative deformation mechanism of the tunnel lining under the long-term dynamic loading of high-speed rail was the opening and dislocation of the joints by using numerical simulation and laboratory tests [11]. Bai et al. analyzed the dynamic response of parallel

\*E-mail address: w\_sr88@163.com



tunnels excavation. The left-hand tunnel was excavated first and then the right-hand tunnel. The excavation of the right tunnel lagged behind that of the left tunnel by 25 m [17].

As seen from Table 1, the surrounding rock of the tunnels mainly related to grades V, and its physical and mechanical parameters were selected according to the China

Code for the Design of Highway Tunnels and the China Guide to the New Austrian Method for Railway Tunnels. As shown in Fig. 4, under the shallow burial conditions (about 14 m), the monitoring points were located at key locations of the middle pillar to observe the dynamic response characteristics of these positions.

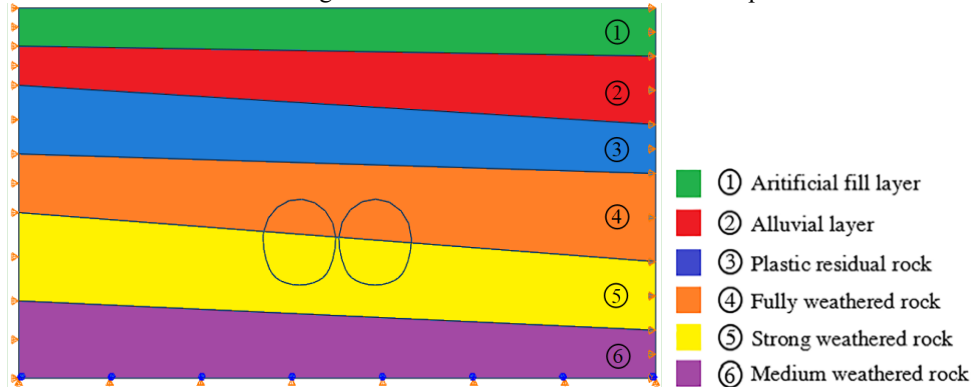


Fig. 3. The computational model and its boundary conditions.

Table 1. Calculating parameters for the model

Grade and structure	Weight (kN/m <sup>3</sup> )	Elastic modulus (GPa)	Poisson's Ratio	Friction angle (°)	Cohesion (MPa)
V	20	0.6	0.38	25	0.08
Lining	25	35.1	0.20	43	1.30
Bedding	25	30.5	0.20	45	1.05

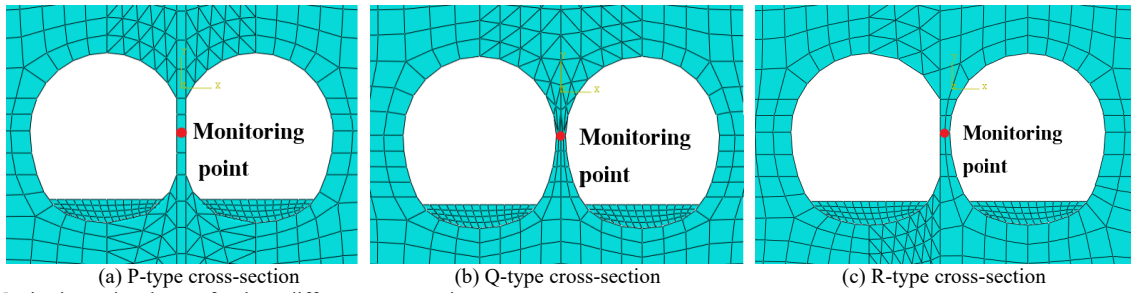


Fig. 4. Monitoring points layout for three different cross-sections.

### 3.2.2 Selection of boundary conditions

The simulation of tunnel excavation, support and train vibration load were divided into six steps. The simulation of tunnel excavation and support was carried out under static conditions. The corresponding boundary conditions were static boundary conditions: the left and right boundary were constrained by X-direction displacement, the bottom boundary was constrained by Y-direction displacement, and the upper boundary was free boundary. In order to eliminate the reflection error of the vibration wave on the boundaries and simulate the characteristics of the infinite boundary of the soil, the viscoelastic boundary condition of the model was adopted in the dynamic calculation process.

Viscoelastic boundary is a kind of artificial boundary condition, which is used to better realize the elastic recovery performance of far-field earth medium in the model of finite boundary. To simulate the propagation law of wave more accurately, Rayleigh damper was used to achieve this purpose in the calculation model, and the expression is as follows:

$$[C] = \alpha[M] + \beta[K] \quad (1)$$

where,  $[C]$ ,  $[K]$ , and  $[M]$  are the damping matrix, the total stiffness matrix, and the mass matrix of the system, respectively.  $\alpha$  and  $\beta$  are the damping parameters.

### 3.3 Theoretical analysis of train vibration loads

#### 3.3.1 Numerical calculation of train dynamic loads

According to the orthogonal condition of mode shapes, the relationship between the undetermined damping parameters and the damping ratio should be as follows:

$$\xi_k = \frac{\alpha}{2\omega_k} + \frac{\beta\omega_k}{2} \quad (k=1, 2, 3, \dots, n) \quad (2)$$

where,  $\xi_k$  and  $\omega_k$  are the damping ratio, the natural frequency of the system, respectively.

The natural vibration characteristics of soil model under the train vibration loads can be obtained by characteristic equation:

$$[K]\{v\} = \lambda[M]\{v\} \quad (3)$$

where,  $\{v\}$  and  $\lambda$  are the eigenvector, the eigenvalue of natural vibration of the system, respectively.

The equation of equilibrium motion of the whole system can be obtained by using the subspace iteration method of Sturm sequence:

$$[M]\{\ddot{\mu}\} + [C]\{\dot{\mu}\} + [K]\{\mu\} = \{F(t)\} \quad (4)$$

where,  $\mu$ ,  $\dot{\mu}$ , and  $\ddot{\mu}$  are the displacement vector, the velocity vector, and the acceleration vector, respectively.  $F(t)$  is the time-varying nodal force vector.

Pan and Pande proposed the Newmark implicit integration method for the calculation of train vibration loads [6]. Therefore, the motion equilibrium differential equation of the model structure system at  $t+\Delta t$  can be expressed as:

$$[M]\{\ddot{\mu}_{t+\Delta t}\} + [C]\{\dot{\mu}_{t+\Delta t}\} + [K]\{\mu_{t+\Delta t}\} = \{F(t + \Delta t)\} \quad (5)$$

Rayleigh damping is adopted in the damping matrix of the model structure:

$$[C] = \alpha[M] + \beta[K] \quad (6)$$

$$\begin{cases} \alpha = \zeta_0 \omega_0 \\ \beta = \frac{\zeta_0}{\omega_0} \end{cases} \quad (7)$$

where,  $\omega_0$  is the base frequency of the system, it can be determined by modal analysis of the model structure.  $\zeta_0$  is the damping ratio of corresponding modes of the system.

According to the principle of Newmark implicit integration, it can be calculated as:

$$\begin{cases} [\ddot{\mu}_{t+\Delta t}] = [\dot{\mu}_t] + [(1-\delta)\ddot{\mu}_t + \delta\ddot{\mu}_{t+\Delta t}]\Delta t \\ [\mu_{t+\Delta t}] = [\mu_t] + \dot{\mu}_t\Delta t + \left[\left(\frac{1}{2}-\gamma\right)\ddot{\mu}_t + \gamma\ddot{\mu}_{t+\Delta t}\right]\Delta t^2 \end{cases} \quad (8)$$

$$\begin{aligned} &\left(\frac{1}{\gamma\Delta t^2}[M] + \frac{\delta}{\gamma\Delta t}[C] + [K]\right)\mu_{t+\Delta t} = [F(t + \Delta t)] + \\ &[M]\left[\frac{1}{\gamma\Delta t^2}\mu_t + \frac{1}{\gamma\Delta t}\dot{\mu}_t + \left(\frac{1}{2\gamma}-1\right)\ddot{\mu}_t\right] + \\ &[C]\left[\frac{1}{\gamma\Delta t^2}\mu_t + \left(\frac{\delta}{\gamma}-1\right)\dot{\mu}_t + \frac{\Delta t}{2}\left(\frac{\delta}{\gamma}-2\right)\ddot{\mu}_t\right] \end{aligned} \quad (9)$$

where, integration constant  $\delta=0.5$ ,  $\gamma=0.25$ , integration step  $\Delta t=T_{\max}/100$ . ( $T_{\max}$  is the maximum period of the system, which is determined by the modal analysis of the structural system).

### 3.3.2 Excitation form of train vibration load

The main reason for the train vibration loads is the wheel factor and the track irregularity. The wheel factors comprise the wheel eccentricity and the wheel flat. The track irregularity mainly includes the track joints and the defective joints, the defects of rail foundation, the track geometry irregularity, etc. The superposition coefficient and dispersion coefficient were introduced to correct the existing train vibration load expression, the vibration load expression is [6]:

$$F(t) = k_1 k_2 (P_0 + P_1 \sin \omega_1 t + P_2 \sin \omega_2 t + P_3 \sin \omega_3 t) \quad (10)$$

where,  $k_1$  (1.2-1.7),  $k_2$  (0.6-0.9) are the superposition coefficient, the dispersion coefficient of wheel and rail

action, respectively.  $P_0$  is the single wheel static load.  $P_1$ ,  $P_2$  and  $P_3$  are the vibration load peaks corresponding to the rail's natural circular frequencies  $\omega_1$ ,  $\omega_2$ , and  $\omega_3$ .

$$P_i = M_0 a_i \omega_i \quad (i=1, 2, 3) \quad (11)$$

where,  $M_0$  is the mass under the spring.  $a_i$  is a typical vector height, whose value is determined according to the British geometric irregularity management value, as shown in Table 2.  $\omega_i$  is the circular frequency of irregular vibration wavelength corresponding to vehicle speed.

$$\omega_i = 2\pi v / L_i \quad (i=1, 2, 3) \quad (12)$$

where,  $v$  is the train speed.  $L_i$  is the typical wavelength.

**Table 2.** Management value of track's geometry unsmooth [18]

Control conditions	Wave length (mm)	Versine (mm)
According to driving smoothness	50.0	16.0
	20.0	9.0
	10.0	5.0
According to dynamic additional load acting on the track	5.0	2.5
	2.0	0.6
	1.0	0.3
Waveform consumption	0.5	0.1
	0.05	0.005

According to the operation standard of high-speed railway tunnel in China, the axle load of the train is 17 t and the mass under the spring is  $M_0=750$  kg. The irregular vibration wavelengths and vector heights corresponding to the three control conditions of comfort, dynamic additional load and waveform wear are  $L_1=10.0$  m,  $A_1=3.5$  mm,  $L_2=2.0$  m,  $A_2=0.4$  mm,  $L_3=0.5$  m,  $A_3=0.08$  mm, respectively. According to the engineering background, the train design speed of Guangzhou Metro Line 3 is 120 km/h. However, due to many factors such as stopping at interval stations and bending of route, the actual speed of train can not reach its designed speed. In this study, the train speed is actually 72 km/h, 90 km/h, and 108 km/h, respectively. According to Eq. (10), the expressions of train vibration loads at three different speeds above mentioned are obtained as follows, and the time history fitting curves are shown in Fig. 5.

$$F(t) = 80 + 0.41\sin(4\pi t) + 1.18\sin(20\pi t) + 3.79\sin(80\pi t) \quad (13)$$

$$F(t) = 80 + 0.64\sin(5\pi t) + 1.85\sin(25\pi t) + 5.92\sin(100\pi t) \quad (14)$$

$$F(t) = 80 + 0.93\sin(6\pi t) + 2.67\sin(30\pi t) + 8.53\sin(120\pi t) \quad (15)$$

## 4. Result and Discussion

### 4.1 Dynamic response analysis of vibration acceleration

The middle pillar is the weakest part of the ultra-small spacing tunnels. The vibration loads generated during train operation will inevitably cause the vibration of tunnel structures, which will affect the stability of the middle pillar, in particular.

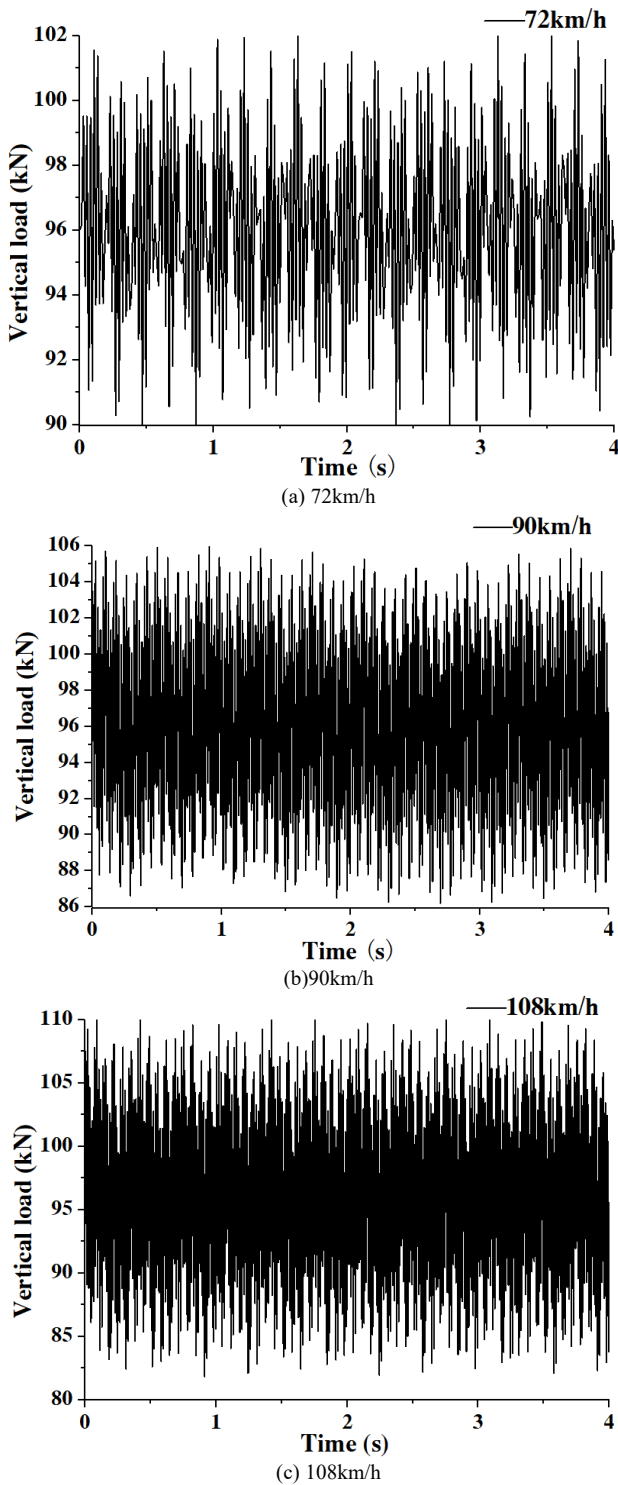


Fig. 5. Time-history fitting curves of train vibration load at different speeds.

As shown in Figs. 6 and 7, the peak vertical accelerations of the monitoring points increase with the train speed increasing for different tunnel cross-sections. For train speed 90 km/h, the vibration acceleration is smaller than that of others speeds. Besides, it can be found that whether the single or double trains run, the vertical acceleration vibration amplitude of P-type cross-section is the largest, that of Q-type cross-section is the smallest, and R-type cross-section is in the middle.

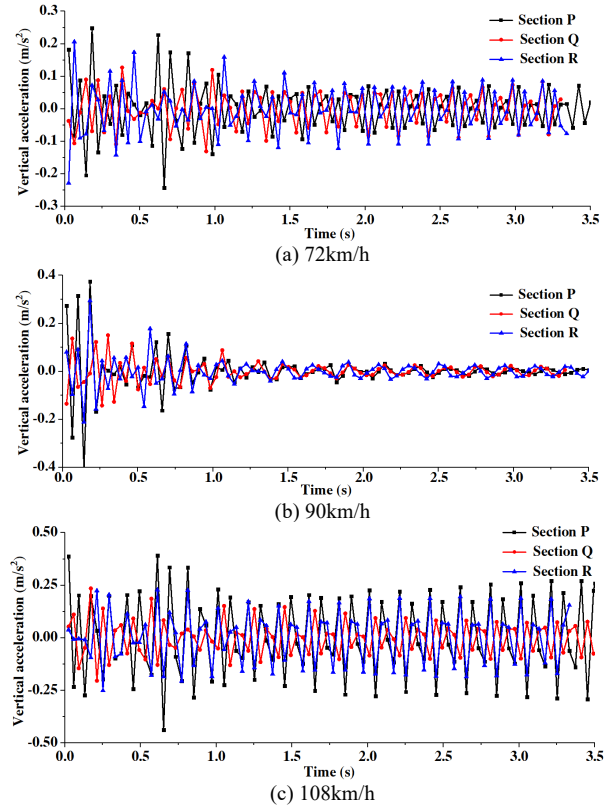


Fig. 6. Vertical accelerations of the monitoring points for three tunnel cross-sections with single train at different speeds.

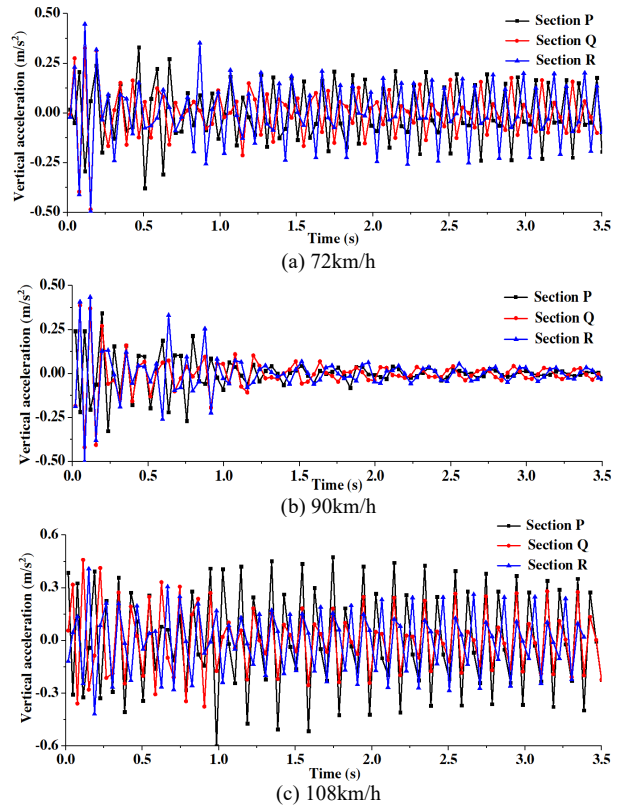


Fig. 7. Vertical accelerations of the monitoring points for three tunnel cross-sections with double trains at different speeds.

#### 4.2 Dynamic response analysis of vibration velocity

It can be seen from Figs. 8 and 9, the vibration velocities of monitoring points increase with the train speed rising, but the vibration velocity of the middle pillar caused by train vibration loads is very small. Besides, both single and double trains operation, the vibration velocities of the middle

pillars for three different tunnel cross-sections on vibration amplitude are slightly different.

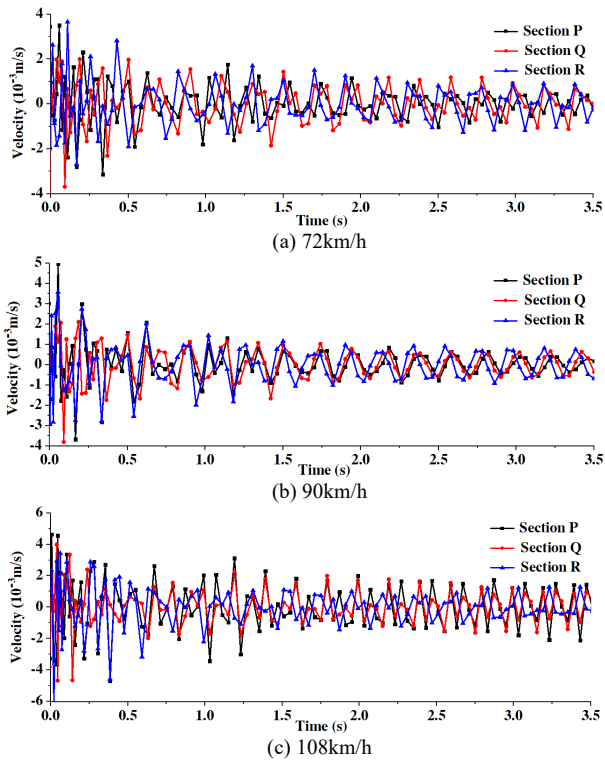


Fig. 8. Velocities of the monitoring points for three tunnel cross-sections with single trains at different speeds.

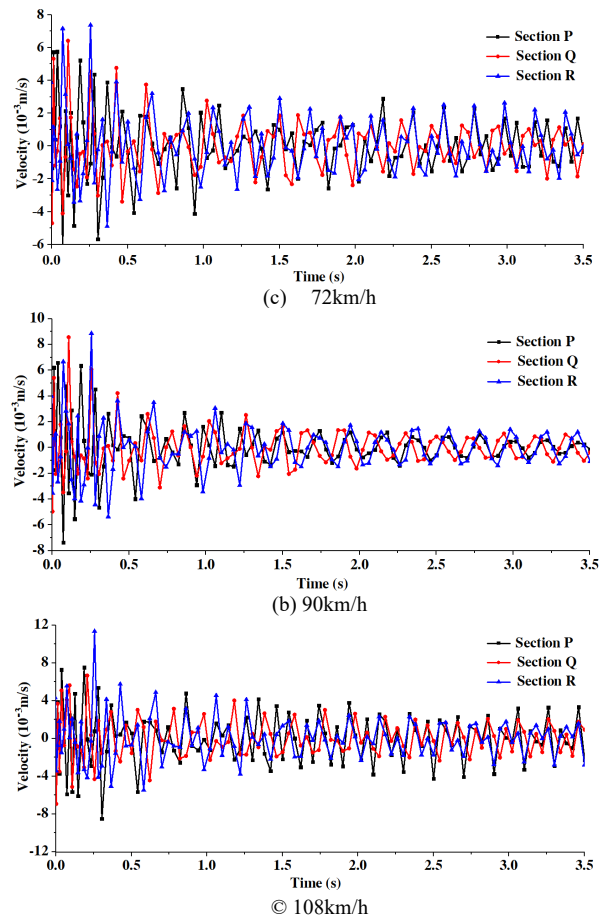


Fig. 9. Velocities of the monitoring points for three tunnel cross-sections with double trains at different speeds.

### 4.3 Dynamic response analysis of vertical displacement

The displacement variation of tunnel structure under train vibration loads is one of the most intuitive manifestations of tunnel stability. Therefore, it is necessary to analyze and discuss the displacement variation rules of tunnel structure during train running.

In Fig. 10, under the vibration load of a single train, the vertical displacements of three tunnel cross-sections are hierarchically distributed. The vertical displacement of R-type tunnel section is the smallest, that of the P-type section is the largest. and Q-type cross-section is in the middle. However, the vertical displacement vibration amplitude of R-section is the largest. It can be calculated from Fig. 11, under the action of the double-train, the vertical displacements of monitoring points in the middle pillar of three tunnel cross-section almost overlap with each other, and the vibration rule is basically the same and the difference is very small.

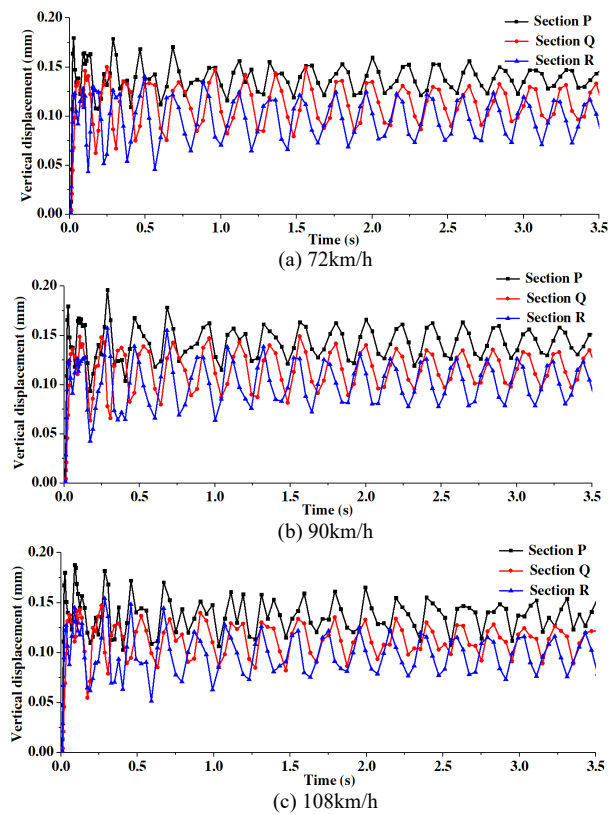
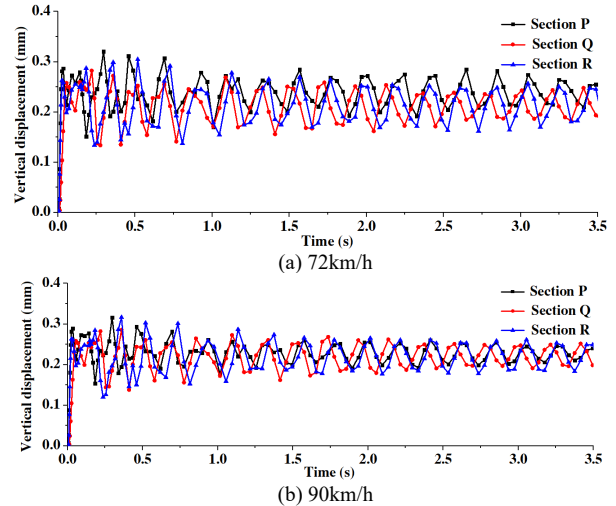


Fig. 10. Vertical displacements of the monitoring points for three tunnel cross-sections with single trains at different speeds.



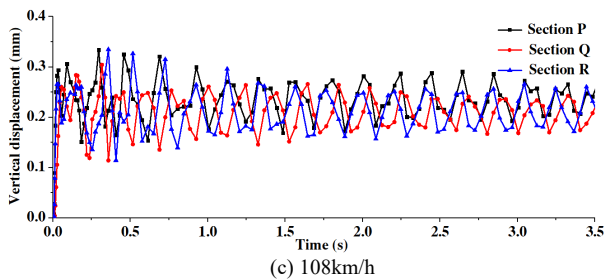


Fig. 11. Vertical displacements of the monitoring points for three tunnel cross-sections with double trains at different speeds.

#### 4.4 Dynamic analysis of horizontal displacement

Fig. 12 implies that the horizontal displacements of monitoring points under the vibration loads of a single train with different train speeds show a slightly difference on values. But the vibration amplitude of the monitoring point of P-type cross-section is the largest, while that of the Q-type and R-type cross-sections are not significantly different.

As shown in Fig. 13, no matter the running speed of the train is high or low, the horizontal displacement vibration amplitude of monitoring point of R-type cross-section is the largest. In addition, the horizontal vibration of monitoring point of P-type and Q-type cross-sections under the vibration load of double-train running is slight, and the vibration curve almost tends to be a straight line.

In summary, due to P-type and Q-type cross-sections are symmetric structure, the horizontal vibration energy waves at waist of the middle pillars are offset each other under the vibration loads of double trains, so the horizontal displacement vibration of the middle pillar is flat. Besides, due to the R-type cross-section is asymmetric structure, which lead to the vibration amplitude of horizontal displacement of the middle pillar being larger.

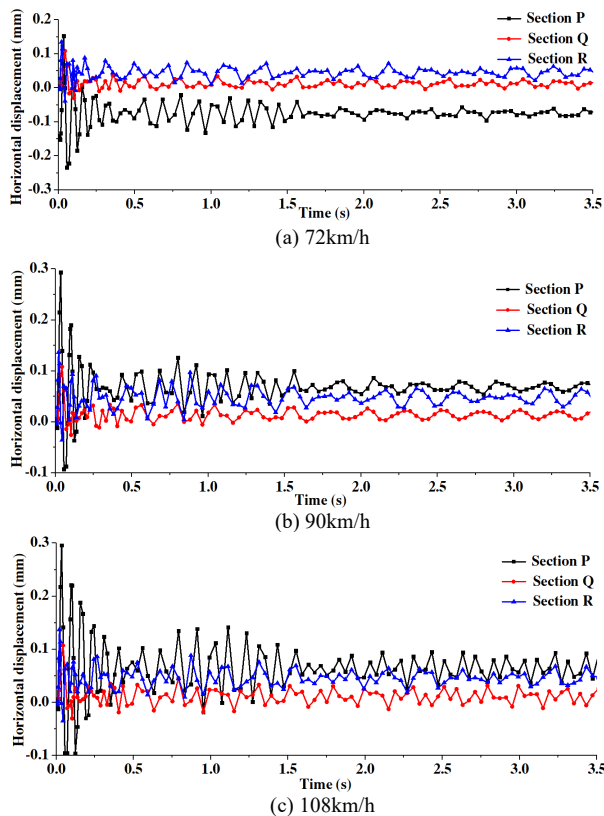


Fig. 12. Horizontal displacements of the monitoring points for three tunnel cross-sections with single trains at different speeds.

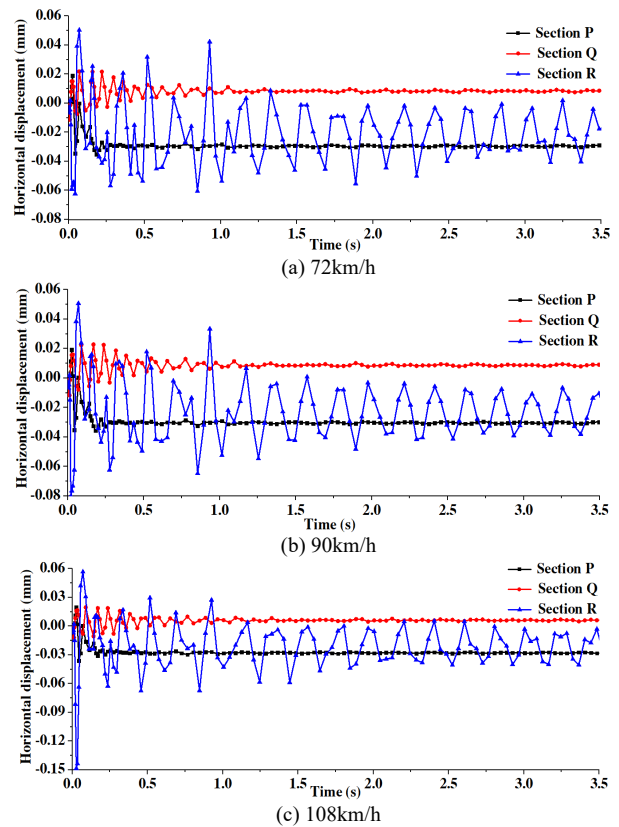


Fig. 13. Horizontal displacements of the monitoring points for three tunnel cross-sections with double trains at different speeds.

#### 5. Conclusions

To study the dynamic response characteristics of the middle pillar in the ultra-small spacing tunnels, the vibration acceleration, velocity, vertical displacement, horizontal displacement of the middle pillar under different train speeds were analyzed and discussed. The conclusions are as follows:

(1) The higher the speed of train travel, the greater the impact on the middle pillar of the ultra-small spacing tunnels. When simulating the dynamic response of tunnel structure under train vibration load in the two-dimensional model, the superposition effect should be considered in the expression of train vibration load excitation.

(2) The dynamic responses of acceleration, velocity, and vertical displacement of the middle pillars in three tunnel cross-sections under the train vibration loads are slightly different. However, compared with the vertical displacement, the horizontal displacement is relatively smaller both in value and vibration amplitude. Furthermore, the dynamic response of the middle pillar in the Q-type tunnel cross-section is the smallest, that of the R-type is the largest, and the P-type is in the middle.

(3) The asymmetric tunnel cross-section of the ultra-small spacing tunnels has a great influence on the dynamic response of the middle pillar, especially in the aspect of horizontal displacement.

Since the practical engineering is actually a three-dimension problem, the three-dimension model, which can reflect the difference between two trains traveling in the same or opposite direction, should be studied in the future.

#### Acknowledgements

This work was financially supported by the National Natural Science Foundation of China (51774112; 51474188), the

International Cooperation Project of Henan Science and Technology Department (182102410060), the Doctoral Fund of Henan Polytechnic University (B2015-67).

This is an Open Access article distributed under the terms of the Creative Commons Attribution License



## References

1. Tian, W., "Dynamic response of tunnel and track structure subjected to metro load and vibration attenuation methods". Master thesis of Tongji university, China, 2007, pp. 3-5.
2. Zhang, Z. Q., Sun, J., Luo, J. Z., Deng, G. H., "Review of the influence of train-induced vibratory load on metro tunnel in loess area". *Journal of Underground Space and Engineering*, 12(S1), 2016, pp. 66-74.
3. Zou, C., "Train-induced vibration transmission and mitigation in metro depot and over-track buildings". Doctoral Dissertation of South China University of Technology, China, 2017, pp. 2-3.
4. Gupta, S., Liub, W. F., Degrandea, G., Lombaerta, G., Liub, W. N., "Prediction of Vibration Induced by Underground Railway Traffic in Beijing". *Journal of sound and vibration*, 310(3), 2008, pp. 608-630.
5. Gupta, S., Van den Berghe, H., Lomberta, G., Degrande, G., "Numerical modelling of vibrations from a Thalys high speed train in the Groene Hart tunnel". *Soil Dynamics and Earthquake Engineering*, 30, 2010, pp. 82-97.
6. Pan, C. S., Pande, G. N., "Preliminary Deterministic Finite Element Study on a Tunnel Driven in Loess Subjected to Train Loading". *Civil Engineering Journal*, 17(4), 1984, pp. 19-29.
7. Zhang, Y. E., Bai, B. H., "The method of identifying train vibration load acting on subway tunnel structure". *Journal of Vibration and Shock*, 19(3), 2000, pp. 68-71.
8. Liang, B., Luo, H., Sun, C. X., "Simulated study on vibration load of high speed railway". *Journal of The China Railway Society*, 28(4), 2006, pp. 89-94.
9. Yang, W. B., Chen, Z. Q., Xu, Z. Y., "Dynamic response of shield tunnels and surrounding soil induced by train vibration". *Rock and Soil Mechanics*, 39(2), 2018, pp. 537-545.
10. Yan, Q. X., Chen, W. Y., Chen, H., Tang, Q. T., Bao, R., Huang, X., "Train vibration response characteristics and damage rule of vertically overlapping shield tunnel in close distance space". *China Railway Science*, 39(4), 2018, pp. 78-84.
11. Yi, H. Y., Qi, T. Y., Qian, W. P., Lei, B., "Influence of long-term dynamic load induced by high-speed trains on the accumulative deformation of shallow buried tunnel linings". *Tunnelling and Underground Space Technology*, 84, 2019, pp. 166-176.
12. Bai, B., Li, C. F., "Three-dimensional Elastic Dynamic Response of Close Crisscross Tunnels Subjected to Subway Loading". *Rock and Soil Mechanics*, 28(S1), 2007, pp. 715-718.
13. Bai, B., Li, C. F., "Elastoplastic Dynamic Responses of Close Parallel Metro Tunnels to Vibration Loading". *Rock and Soil Mechanics*, 30(1), 2009, pp. 123-128.
14. Xu, H. Q., Fu, Z. F., Liang, L. G., Wang, G. B., Chen, L., "Ambient vibration analysis of adjacent perpendicular multi-tunnels under train loads". *Rock and Soil Mechanics*, 32(6), 2011, pp. 1869-1873.
15. Guo, C. X., Wang, K. Y., Li, F. N., "3D-Numerical analysis of dynamic influence of vibrating load on intersecting tunnel structure". *Highway*, 61(4), 2016, pp. 265-270.
16. Wang, X. q., Yang, L. D., Zhou, Z. G., "Dynamic response analysis of lining structure for tunnel under vibration loads of train". *Journal of Rock Mechanics and Geotechnical Engineering*, 25(7), 2006, pp. 1337-1342.
17. Wang, S. R., Shi, K. P., Chen, W. X., Liu, S. P., "Stability analysis of middle rock pillar and cross-section optimization for ultra-small spacing tunnels". *Journal of Engineering Science and Technology Review*, 11(3), 2018, pp. 147-153.
18. Liang, B., Cai, Y., "Dynamic analysis on subgrade of high speed railways in geometric irregular condition". *Journal of the China Railway Society*, (2), 1999, pp. 93-97.